Title
The influence of residual stress on fatigue crack growth rates of additively manufactured Type 304L stainless steel

Authors
Smudde, Christine M
D'Elia, Christopher R
San Marchi, Christopher W
et al.

Publication Date
2022-09-01

DOI
10.1016/j.ijfatigue.2022.106954

Peer reviewed

The Influence of Residual Stress on Fatigue Crack Growth Rates of Additively Manufactured Type 304L Stainless Steel

Christine M. Smudde[1], Christopher R. D'Elia[2], Christopher W. San Marchi[3], Michael R. Hill[2], Jeffery C. Gibeling[1]

[1] Department of Materials Science and Engineering, University of California, Davis

[2] Department of Mechanical and Aerospace Engineering, University of California, Davis

[3] Sandia National Laboratories, Livermore, California

Corresponding Author: Christine M. Smudde
Department of Materials Science and Engineering
University of California
One Shields Ave.
Davis, CA 95616, USA
Phone: (714) 356-0477
Email: cmsmudde@ucdavis.edu

Abstract:

To examine the influence of residual stress on mechanical performance, specifically fatigue crack growth resistance, of additively manufactured (AM) Type 304L stainless steel produced by directed energy deposition (DED) was evaluated and compared to that of conventional wrought Type 304/304L stainless steel. Increasing and decreasing alternating stress intensity factor (ΔK) tests were used to assess fatigue crack growth behavior over a range of crack growth rates in the near threshold regime ($<10^{-8}$ m/cycle). Bulk residual stress and residual stress intensity factor (K_{res}) profiles of a fatigue specimen were measured using the incremental slitting method. Tensile residual stress at the edges of the DED materials led to positive values of K_{res} and faster fatigue crack growth rates in the DED material as compared to wrought material at the same applied ΔK. Correcting for the effects of K_{res} and crack closure in DED Type 304L and commercially available wrought Type 304/304L stainless steel shows that fatigue crack growth rates are similar at values of ΔK lower than 6 $MPa \cdot m^{0.5}$ when compared to rates in wrought material.

Keywords:

Additive manufacturing (AM), directed energy deposition (DED), residual stress, fatigue crack growth, stainless steel

1. *Introduction*

Additive manufacturing (AM) has the potential to revolutionize the production of low volume components for engineering applications. The controlled deposition of material offers the opportunity to produce complex near net shape components on demand that would otherwise be difficult or impossible to create with conventional manufacturing processes. However, before AM materials can expand into structural engineering applications at a large scale, characterization of their mechanical performance, specifically fatigue resistance, is required [1, 2]. Of particular concern to fatigue performance is the fact that even the highest density AM parts exhibit evidence of defects in the as-built condition [3]. Therefore, a damage tolerant design approach, where all materials are assumed to contain defects [4], is essential to the adoption of AM components in structural applications. In damage tolerant design, a thorough understanding of material fatigue crack growth rate behavior is critical to accurately predicting service life under conditions where fatigue resistance is a critical property.

Developing a description of the fatigue performance of additively manufactured materials that is unbiased by the manufacturing process and that can be compared to current certification standards for conventionally processed materials is a significant challenge. The unique microstructure formed during layer deposition and the residual stress induced by the intense thermal gradients of the AM process contribute to noticeable differences in fatigue behavior, especially near the threshold of crack growth rates ($<10^{-8}$ m/cycle) [5, 6]. In this regime, where the applied loads of a traditional fatigue crack growth test are low, microstructural contributions to crack path behavior may influence the crack growth rates by promoting a tortuous crack path or enabling premature crack face contact in the crack wake. In addition, the influence of residual stress on fatigue crack growth is amplified near the threshold regime, where the contributions from residual stress to the crack growth driving force approach the values of the applied K_{min} and K_{max}.

The influence of microstructure (grain size and morphology) and bulk residual stress on the fatigue crack growth behavior in additively manufactured materials is not well described in the literature. Studies focused on microstructure of AM materials have shown that there is an orientation dependence of the fatigue crack growth behavior due to the anisotropic microstructure of AM materials. Specifically, fatigue crack growth rates differ depending on the orientation of the applied loading relative to the build direction in the Paris and threshold regimes [7-11]. Near surface measurements have revealed that the residual stress at the edges of the AM material are tensile [10], but the influence of residual stress on the fatigue crack growth behavior has not been assessed Other studies have focused specifically on quantifying manufacturing-induced residual stress in AM materials. For example, in directed energy deposition (DED) material, high uniaxial macroscale (bulk) residual stress directed along the build direction has been determined to have tensile values at the edges and compressive values in the center of the build [12]. However, while the magnitude of residual stress could be minimized by controlling the processing parameters, elimination of residual stress requires post-processing heat treatment, but at the expense of reducing strength. Therefore, it seems essential to understand the influence of process-induced residual stress on the fatigue performance of DED materials.

Quanitfying the effects of residual stress in fatigue crack growth data is necessary to reveal the intrinsic fatigue resistance of DED material. By determining the residual stress intensity factor, K_{res}, which characterizes the contribution of residual stress at the crack tip to the total driving force of crack growth, corrections can be made to fatigue crack growth data. In the case of tensile residual stress, where the crack is considered open, the effective value of the stress intensity factor is found by the superposition of K_{res} and K_{app}. Donald and Lados developed a method for correcting for residual stress by considering the contributions of K_{res} on the minimum (K_{min}) and maximum (K_{max}) stress intensity factors as a mean stress effect, resulting in a corrected alternating stress intensity factor, ΔK_{corr} [13]. Few researchers have utilized the ΔK_{corr} method when evaluating materials with residual stress [14, 15]. To date, the application of this method to AM materials has not been published in the literature.

The objective of this study is to determine the fatigue crack growth behavior of DED Type 304L stainless steel independent of the influence of residual stress by quantifying and correcting for K_{res}. The incremental slitting method was used to determine values of K_{res} as a function of crack length in a compact tension fatigue crack growth specimen machined from as-built DED material. Decreasing applied ΔK tests were used to explore the near threshold fatigue crack growth rates less than 10^{-8} m/cycle in the DED material. When the crack growth rates reached a predetermined level of approximately 2-3 x 10^{-10} m/cycle , the tests were continued under constant applied load amplitude conditions to gain insight into the consistency of the fatigue data under ΔK increasing conditions as described in ASTM E647 [16]. Commercially available wrought Type 304/304L material was tested under the same conditions to establish a baseline for fatigue crack growth behavior in typical material. Then, a corrected stress intensity (ΔK_{corr}) analysis method was used to account for the effects of K_{res} on fatigue crack growth rate data. In this manner, the instrinsic fatigue crack growth rates of DED Type 304L stainless steel, independent of residual stress, were characterized.

2. Material and methods

2.1. Material

The Type 304L stainless steel under evaluation was additively manufactured via directed energy deposition (DED) in a Laser Engineered Net Shaping (LENS®) 750 workstation utilizing the time-invariant processing input parameters listed in Table 1. A hatch scan pattern that alternated 90 degrees with each layer was utilized during the build process. Gas atomized austenitic stainless steel powder of size 45 µm to 105 µm was used in the deposition process and the chemical composition for the powder as determined by Smith et al. for replicate builds made on the same equipment [17] is given in Table 2, showing that the powders conformed to standard requirements of 304L grade alloys [18]. Solution annealed commercially available wrought Type 304/304L stainless steel was used for comparison. The chemical composition of the dual certified Type 304/304L is included in Table 2. The small differences in chemical composition are assumed to have negligible influences on fatigue crack growth behavior in this study.

Table 1: Processing Parameters for DED Type 304L Stainless Steel

Processing Parameter:	**Value:**
Laser power	Yb:fiber 450 W
Laser scan speed	10 mm/s
Hatch increment	0.64 mm
Layer increment	0.20 mm
Oxygen concentration	< 5 ppm
Powder size	45-105 µm

Table 2: Composition (wt%) of bulk wrought Type 304/304L gas atomized Type 304L feedstock powder.

	Fe	**Cr**	**Ni**	**Mn**	**Mo**	**N**	**C**	**Si**	**O**	**S**	**P**	**Cu**
Wrought 304/304L	Bal	18.03	8.14	1.80	0.37	0.072	0.023	0.27	-	0.001	0.036	0.43
DED 304L	Bal	19.1	10.6	1.50	0.07	0.010	0.015	0.60	0.023	0.003	0.005	-

Processing parameters were optimized for greater than 99% density in the DED material. Mechanical tests in similar builds made on the same equipment with the same processing parameters previously exhibited yield strength of 320 MPa for the longitudinal direction, ultimate tensile strength of 620 MPa, and total elongation to failure of 72% [17]. Additionally, large area electron back-scatter diffraction (EBSD) images of the DED Type 304L microstructure demonstrated anisotropic grain shapes that were elongated in the build direction [17]. Replicate vertical wall builds with nominal dimensions of 107 mm x 55.9 mm x 7.62 mm were deposited on individual wrought stainless steel baseplates of dimension 152 mm x 152 mm x 6.35 mm (Figure 1). Material for fatigue testing and analysis was isolated by first removing the vertical wall builds from the baseplate via wire electrical discharge machining (EDM) (solid line). Then, a thin segment of material from the side of each wall was removed by EDM prior to the machining of fatigue crack growth testing specimens (dashed line), leaving a plate of material 106 mm (along the build direction) by 38 mm.

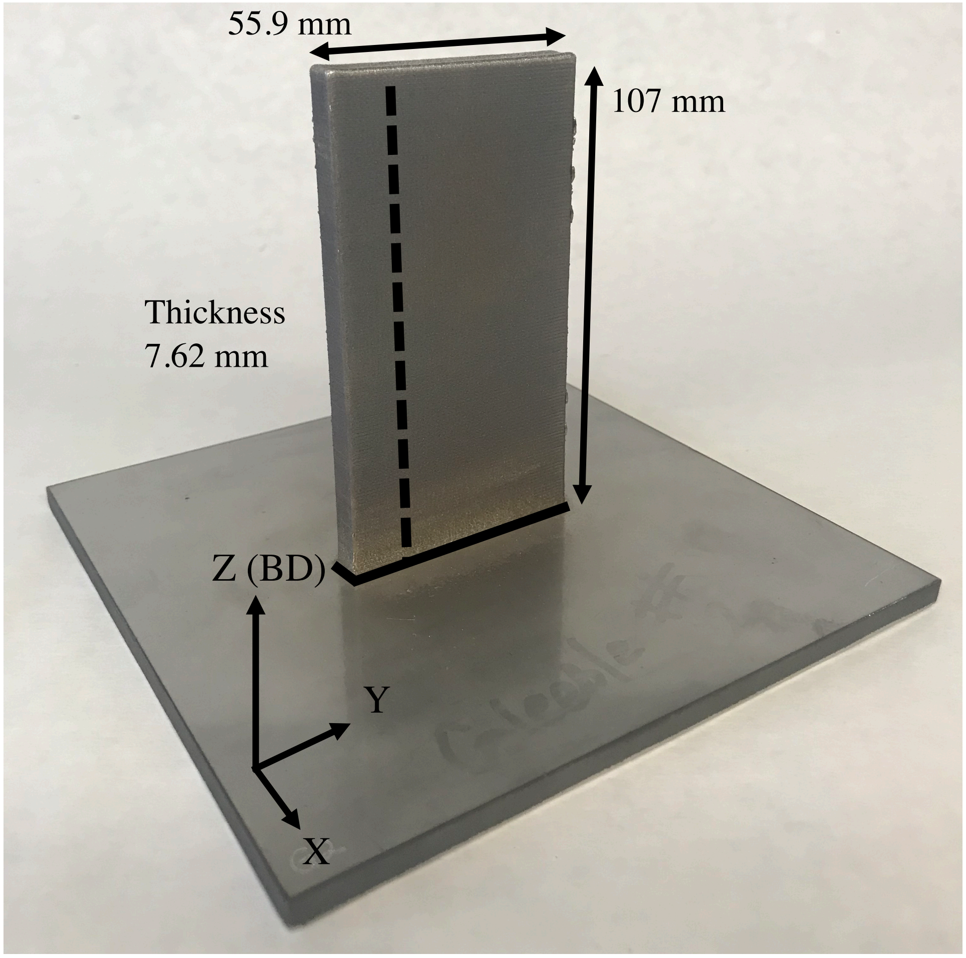

Figure 1: Image of DED vertical wall build with black lines showing the locations of EDM material removal.

From each plate of the two vertical wall builds (Figure 2), three compact tension (C(T)) fatigue crack growth specimens were extracted to evaluate fatigue crack growth behavior in the near threshold regime. A total of five specimens with the loading axis oriented parallel to the build direction (BD) were used in this study and were differentiated by their build number (DED1 and DED2) and by their extraction location (bottom (B), middle (M), and top (T)) as seen in Figure 2. C(T) specimens were machined with thickness (B) of 6.35 mm and width (W) of 26.4 mm. Prior to fatigue testing, a notch was introduced to all specimens by wire EDM to a nominal crack length, a_n, of 5.1 mm in compliance with ASTM E647 [16]. The top and bottom specimens from both DED1 and DED2 were subjected to fatigue crack growth testing, while the middle specimen from DED1 was reserved for residual stress measurement using the incremental slitting method.

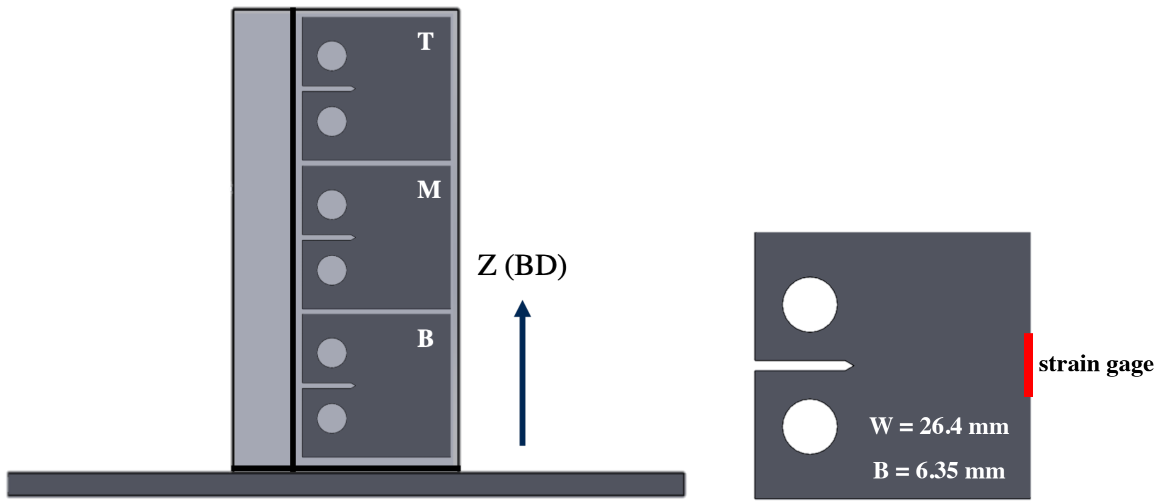

Figure 2: Schematic of C(T) specimen extraction from vertical wall build.

2.2. Residual Stress Evaluation

Residual stress was measured in the DED material using the incremental slitting method. Build-direction residual stress was measured as the C(T) specimens were extracted from the DED plates. After C(T) specimens were completed, the C(T) specimen from the middle of vertical wall build DED1 (DED1-M) was reserved for residual stress analysis. Residual stress was measured prior to the introduction of a fatigue starter notch at the same plane as crack propagation in fatigue tests. The residual stress normal to the crack plane and acting to open the crack was determined as a function of position from the front face of the specimen (x).

The slitting method is a one-dimensional mechanical relaxation technique for determining average through thickness residual stress normal to a plane of interest. Incremental cutting along the plane results in a redistribution of residual stress and strains which are recorded by a strain gage applied at the back face. An inverse analysis is performed using the strain from each cut increment to determine the average through thickness normal residual stress. In the present work, a strain gage was applied at the back face and incremental slitting was performed by wire EDM using 0.381 mm fixed depth increments to 29.5 mm from the front face or 90% of the total specimen width (1.25W) [19]. Strain was measured at each cut increment and residual stress was determined using the pulse-regularization inverse analysis technique [20]. The slitting measurement rendered DED1-M unavailable for fatigue testing.

To evaluate the contribution of residual stress to the stress intensity factor, values of K_{res} acting in the crack plane are determined from the strain data collected during the incremental slitting method. The residual stress intensity factor, K_{res}, is determined as a function of crack size as measured from the load line, a* (a* = x - 0.25W). The fitted strain values and a geometry dependent influence function (Z(a*)) as described by Schindler [21] and further developed by Olson for the C(T) geometry [22] were used in Equation 1 to determine K_{res}:

$$K_{res}(a^*) = \frac{E}{Z(a^*)} * \frac{d\varepsilon(a^*)}{da} \quad (1)$$

Here E is the elastic modulus of a fully dense austenitic stainless steel, 200 GPa, and a^* is measured from the load line. The derivative of the strain with respect to the crack length is determined by differentiating a localized curve fit of the strain data. A schematic of the incremental slitting method can be seen in Figure 3.

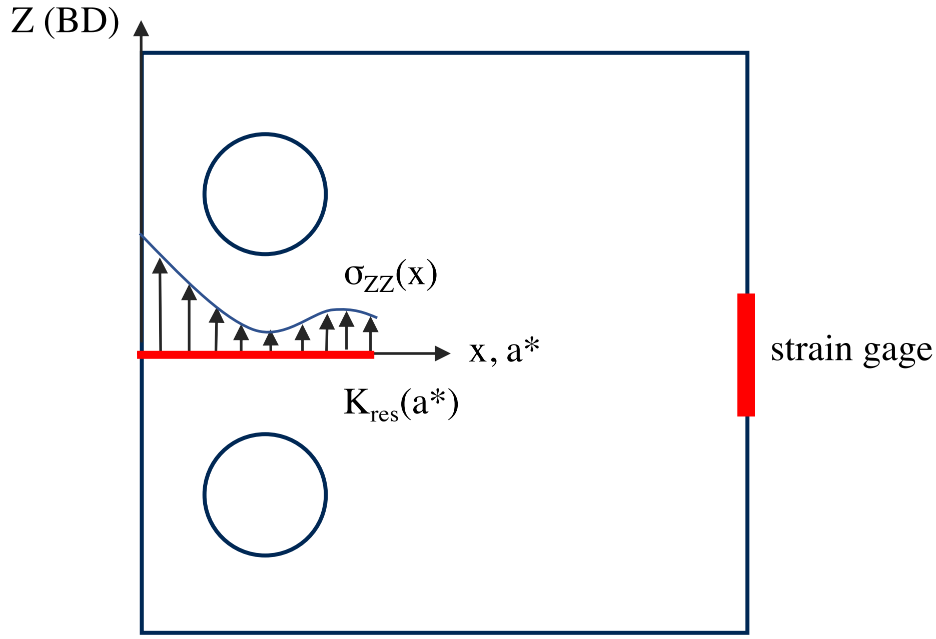

Figure 3: Schematic of incremental slitting method.

To compare the value of K_{res} at the end of the notch depth, the residual stress intensity factor was determined during the notch cutting using the incremental slitting method similar to the process as described for DED1-M. This method was applied to the two bottom C(T) specimens (DED1-B and DED2-B) as well as two wrought C(T) specimens, to assess residual stress in the DED and wrought material. The top specimens (DED1-T and DED2-T) were notched without measuring their residual stress intensity factor.

2.3. Fatigue Crack Growth Testing

Fatigue crack growth testing consistent with the methodology described in ASTM E647 (long cracks) [16] of DED and wrought material was performed on an Instron 1331 servo-hydraulic load frame controlled by a MTS TestStar system. MTS 790.40 fatigue crack growth software was used to execute the tests under K-control conditions at an applied stress ratio of 0.1 and frequency of 10 Hz. For crack length monitoring during the fatigue test, the back-face strain compliance method facilitated data collection of compliance data with high accuracy for post testing analysis. A Micro-Measurements CEA-09-062UWA-350 strain gauge was centered on the crack plane on the back-face of each C(T) specimens as shown in Figure 2 and strains were measured using a Vishay Instruments P3500 strain indicator. The MTS software was adapted to accept a back-face strain input for the compliance method of determining crack length; the absolute value of the measured strain was multiplied by the specimen width to create a modified strain value that is nominally equivalent to the crack opening displacement at the front face location in ASTM E647 compliance equations. Back face strain coefficients were entered into the compliance calculation for crack length in the MTS software [16]. During the fatigue crack growth tests, load and modified strain data with 500 data points per cycle were recorded at 0.05 mm crack increments. A modulus of 200 GPa was consistently employed in the compliance analysis for the materials in this study.

Prior to testing, all specimens were ground to 240 grit and one side was polished to enable visual confirmation that the crack path remained straight. Then, the top and bottom specimens from each build were precracked by an increment in crack length of Δa = 1.3 mm (to a/W = 0.25) using a load shedding methodology incorporated in the MTS TestStar software. The final K_{max} of the precrack was less than the K_{max} at the start of the test in accordance with the ASTM E647 standard [16]. Decreasing applied ΔK tests with a starting K_{max} of 11 MPa· $m^{0.5}$ and a load shedding parameter, *c*, of -0.08 mm^{-1} were then used to probe the near threshold crack growth behavior. When the crack growth rates reached values of 2-3 x 10^{-10} m/cycle, the tests were continued at a constant applied load amplitude, resulting in an increasing applied ΔK test. In this manner, the consistency of the fatigue crack growth behavior as a function of loading condition (i.e., ΔK decreasing compared to ΔK increasing) was evaluated for the DED material. To provide data for comparison, similar tests were conducted on solution annealed wrought Type

304/304L stainless steel (Wrought1,2,3) with mechanical properties reported as yield strength of 320 MPa and ultimate tensile strength of 600 MPa in compliance with ASTM standard A240 [18]. In addition, residual stress was anticipated to be negligible (K_{res} = 0) in the wrought material.

2.4. K_{corr} Method to Correct Fatigue Data for Residual Stress

The methodology outlined by Donald and Lados to correct for varying residual stress effects in fatigue crack growth data was used to transform the fatigue data of DED material [13]. Since residual stress contributes to both the maximum and minimum total stress intensity factors, a fatigue crack growing through a material with a residual stress field experiences a varying total stress ratio (R_{tot}) even when the applied stress ratio (R_{app}) is kept constant. Adding the K_{res} values from the incremental slitting of DED1-M to the applied K_{min} and applied K_{max} of the fatigue crack growth tests gives R_{tot} as a function of crack length (Equation 2):

$$R_{tot}(a) = \frac{K_{min,app}(a)+K_{res}(a)}{K_{max,app}(a)+K_{res}(a)} \tag{2}$$

Normalized stress intensity factor data, ΔK_{norm}, uses a material specific normalization parameter, *n,* to eliminate the effects of varying total stress ratios due to residual stress as given in Equation 3:

$$\Delta K_{norm}(a) = \Delta K_{eff}(a)^{1-n} * \left(K_{max,app}(a) + K_{res}(a)\right)^{n} \tag{3}$$

The adjusted compliance ratio (ACR) method outlined in the appendix of ASTM Standard E647 [16] was used to remove the influence of crack closure on measured fatigue crack growth rate data. The ACR method uses the compliance data to determine the deviation from linearity imposed by contact stresses in the crack wake at low applied loads and correct for crack closure while including the influence of crack tip strain [23]. The resulting value of ΔK is the effective stress intensity factor range ($\Delta K_{ACR} = \Delta K_{eff}$) free of the influence of crack closure needed to compute ΔK_{norm} in Equation 3.

Values of ΔK_{norm} were then further modified to reflect growth rates at the applied stress ratio, R_{app}, of 0.1 using the Walker relationship [24], as expressed in Equation 4:

$$\Delta K_{corr}(a) = \Delta K_{norm}(a) * \left(1 - R_{app}\right)^{n} \quad (4)$$

The value of the normalization parameter, *n*, in Equations (3) and (4) was determined for the DED material using decreasing ΔK fatigue crack growth test data of wrought Type 304/304L. A single C(T) specimen (Wrought4) was tested at three R_{app} values of 0.1, 0.3, and 0.5 to assess fatigue crack growth rates for a range of applied ΔK values and to provide the necessary data to determine the normalization parameter, *n*. In the absence of residual stress, ΔK_{norm} collapses data tested at different R_{app} values onto a single fatigue crack growth rate curve.

3. *Results*

3.1. Residual Stress and K_{res}

Incremental slitting measurements performed during specimen extraction were used to further verify consistency in residual stress throughout the DED material. Measurements performed between bottom (B) and middle (M) specimens (DED-b) and between middle (M) and top (T) specimens (DED-t) are shown in Figure 4. The expected parabolic residual stress profile across the width of the DED material is slightly shifted due to the asymmetrical removal of material prior to specimen extraction.

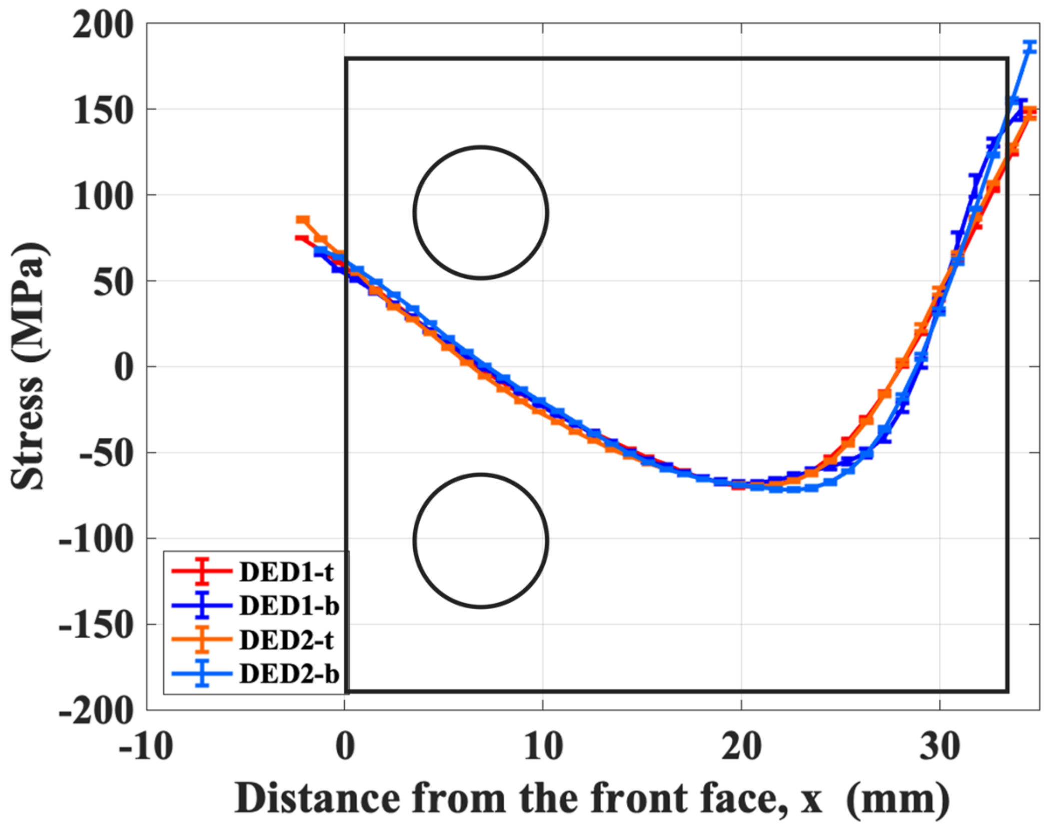

Figure 4: Residual Stress as a function of position from the front face (x) from incremental slitting during specimen extraction with a C(T) specimen geometry superimposed.

The residual stress acting in the C(T) specimen as a function of position from the front face (x) from the incremental slitting measurement on DED1-M is shown in Figure 5. The tensile residual stress decreases at relatively constant slope from the front face of the specimen towards compressive residual stress, with an inflection between 5 and 10 mm from the front face. The inflection is attributed to the machined holes in the C(T) specimen geometry, which interrupts the expected parabolic residual stress profile of the DED material. The peak compressive residual stress occurs around 23 mm from the front face, with the residual stress continuously increasing towards tensile values at positions approaching the back face of the specimen (x > 25 mm).

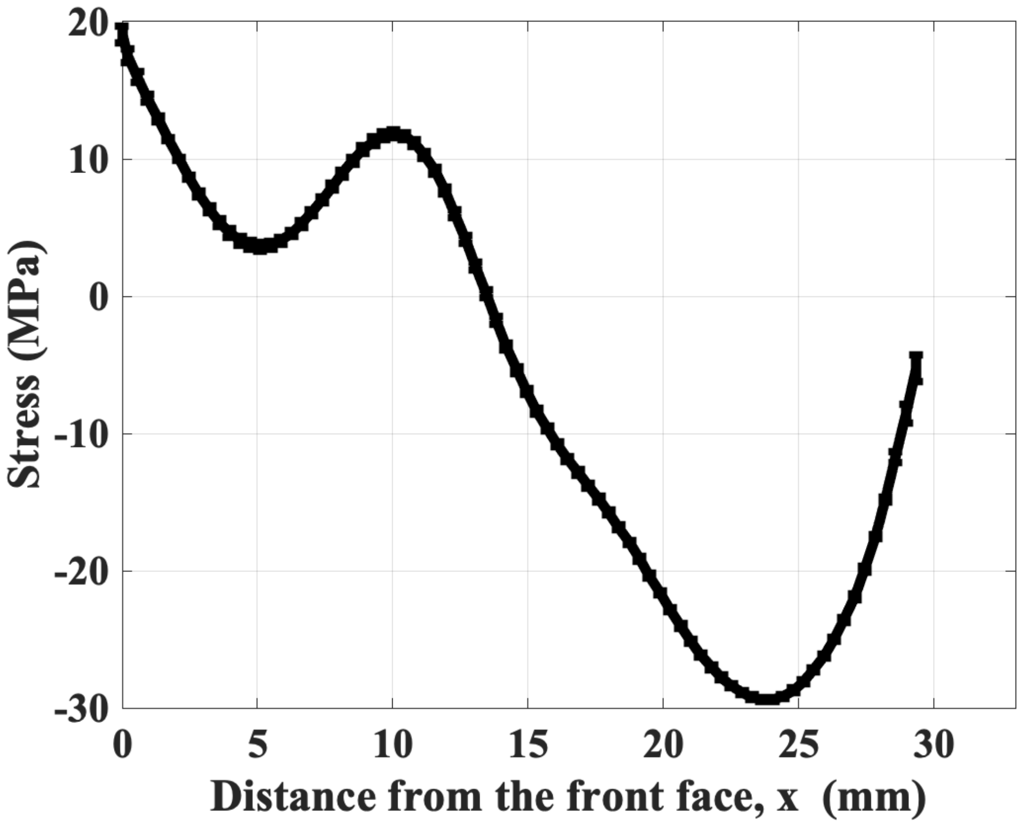

Figure 5: Residual Stress as a function of position from the front face (x) in DED1-M from incrmental slitting.

The corresponding residual stress intensity factor determined from the slitting measurement as a function of crack size as measured from the load line, a*, is plotted in Figure 6. Tensile residual stress near the front face of the DED specimen (Figure 5) leads to positive values of K_{res} throughout the entire range of crack size (Figure 6). The vertical lines in Figure 6 mark the location of the notch tip (solid line) and the crack tip after precracking (dotted line). Results show that crack growth during the fatigue tests would begin with a maximum tensile K_{res} that decreases monotonically as crack length increases. Tensile residual stress intensity should contribute to higher fatigue crack growth rates and lower fatigue thresholds when compared to tests in a residual stress-free material of the same composition and microstructure.

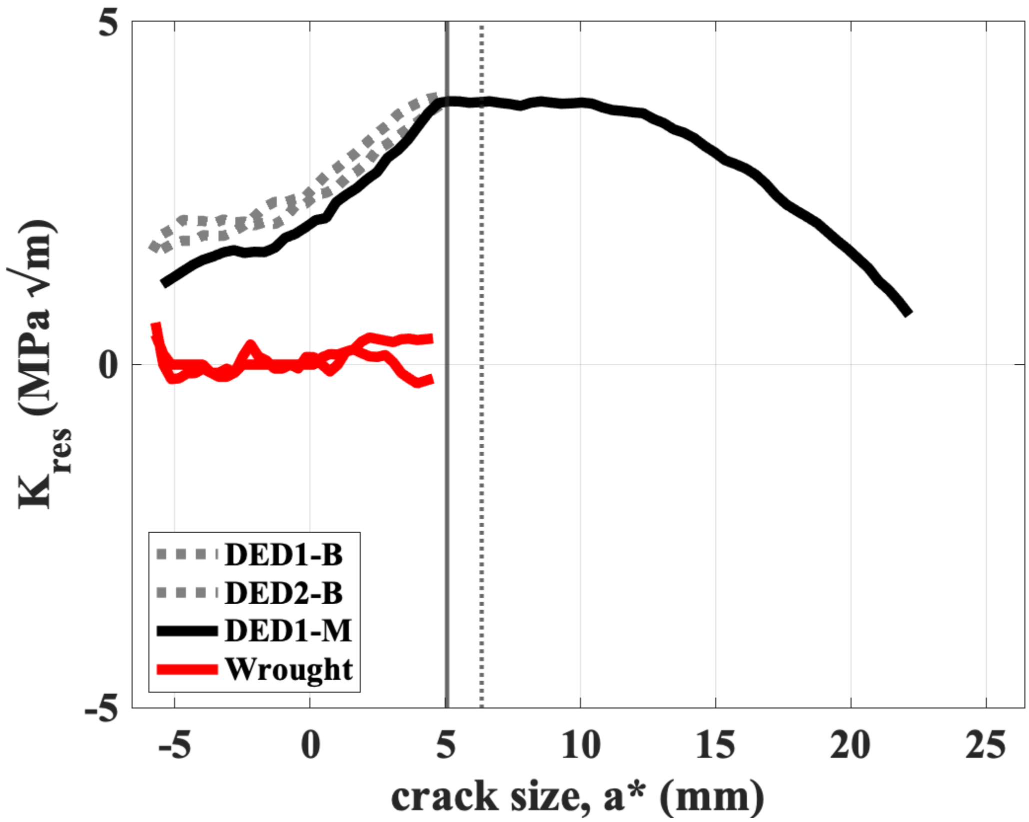

Figure 6: K_{res} as a function crack size for DED Type 304L and wrought Type 304/304L C(T) specimens.

Figure 6 also includes K_{res} values from the notching of the bottom DED C(T) specimens (DED1-B and DED2-B) and two wrought specimens (Wrought1,2). All the DED specimens exhibited a K_{res} value of about 4 MPa·m$^{0.5}$ at the end of the notch, suggesting that the residual stress is relatively similar at each build height sampled in the present work and the incremental slitting results of DED1-M can be used to estimate the K_{res} values of all DED specimens under evaluation. In addition, K_{res} for the wrought specimens verifies the expected negligible residual stress.

3.2. Fatigue Crack Growth Results

Before fatigue crack growth data were analyzed, the validity of the modified strain compliance method for measuring crack length was verified. The fracture surface of a wrought specimen can be seen in Figure 7(a) and the fracture surface of DED1-T can be seen in Figure 7(b). Crack length was measured using ImageJ [25] analysis on the photos in Figure 7 using an average of nine equally spaced positions through the thickness. Measured crack lengths agreed with the values for crack length calculated by the test control software to better than 0.050 mm, which is within the requirements of ASTM E647 [16]. Furthermore, the cracks in both specimens grew straight as defined by the standard.

a)

b)

Figure 7: Fracture surfaces of (a) Wrought Type 304/304L (Wrought1) and (b) DED Type 304L (DED1-T).

The results of the ΔK decreasing and ΔK increasing fatigue crack growth tests for all specimens are plotted in Figure 8 as a function of the applied (non-corrected) ΔK. Fatigue crack growth rates for three wrought specimens with negligible residual stress are plotted for comparison. Since the first specimen (Wrought1) demonstrated equivalent fatigue crack growth data for ΔK decreasing and ΔK increasing, the remaining two wrought specimens (Wrought2,3) were tested only in ΔK decreasing conditions. The data show fatigue crack growth rates in DED are higher than those in wrought, with the largest differences at lower applied ΔK. The higher fatigue crack growth rates in DED are consistent with the positive values of K_{res} (Figure 6) determined for the DED material.

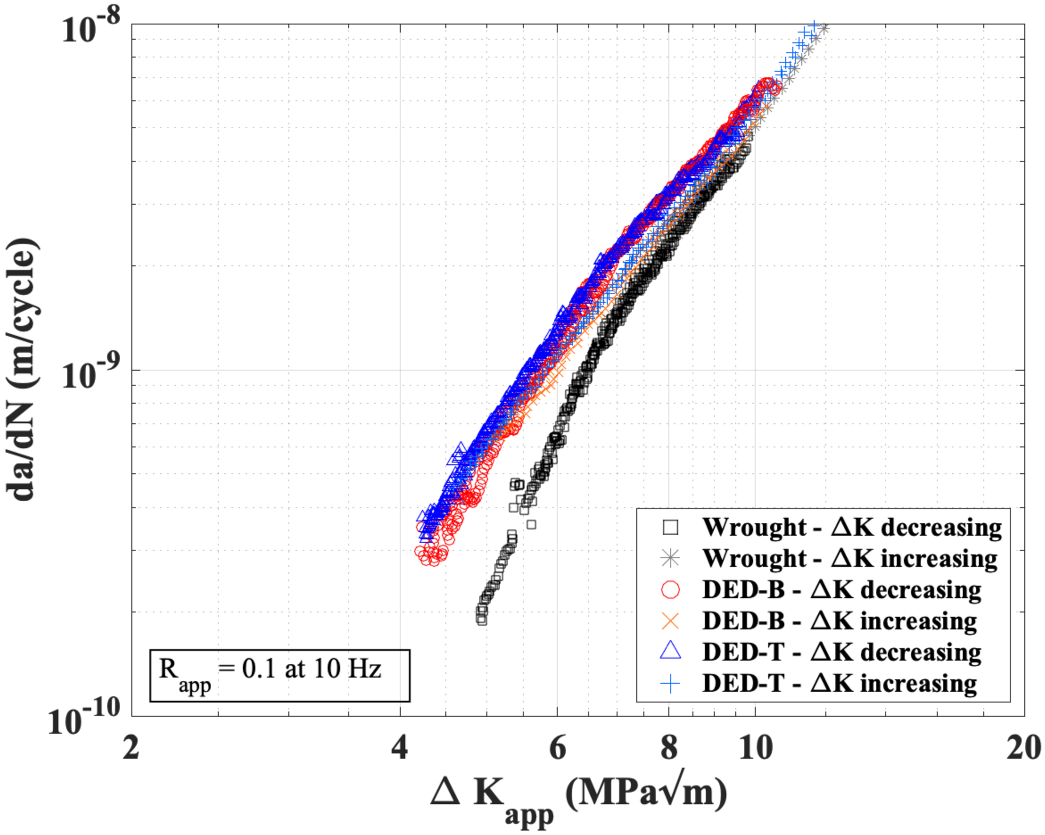

Figure 8: Fatigue crack growth rates (da/dN) vs ΔK_{app} for DED Type 304L and wrought Type 304/304L stainless steel.

3.3. Fatigue Crack Growth Assessment of Wrought Type 304/304L

The wrought Type 304/304L stainless steel with negligible residual stress (K_{res} = 0) was used to provide fatigue crack growth rate data for comparison with the DED Type 304L. The absence of residual atress in the wrought material also allows the determination of the normalization parameter, *n,* which is assumed to be the same for the wrought and DED stainless steel materials. Fatigue crack growth rates at different R values versus ΔK_{app} are presented in Figure 9(a) while Figure 9(b) shows fatigue crack growth rates versus $\Delta K_{ACR.}$ Correcting the data for crack closure was necessary to find the effective values of ΔK, which were needed for the calculation of ΔK_{norm} in Equation 3.

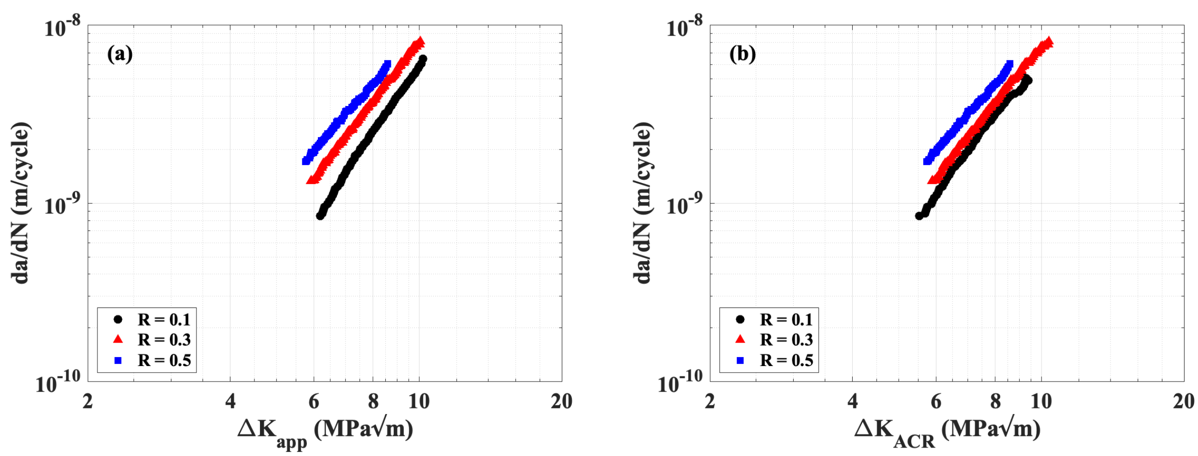

Figure 9: Fatigue crack growth rates (da/dN) versus $\Delta K_{applied}$ (a) and ΔK_{ACR} (b) in wrought 304/304L stainless steel for different applied stress ratios.

The biggest change between the two plots is a shift to the left in the data for R_{app} of 0.1 in Figure 9(b) as compared to Figure 9(a). The shift is consistent with a correction for crack closure in the fatigue crack growth data. The negligible difference between ΔK_{app} and ΔK_{ACR} for data at R_{app} of 0.3 and 0.5 is due to the negligle crack closure at these higher stress ratios.

To determine the appropriate value of *n,* ΔK_{norm} was calculated using the effectice crack growth data in Figure 9(b) using a range of values, *n* = 0.15 to 0.35. The normalization parameter value, n = 0.25, was visually identified to best collapse the data into a single curve (Figure 10), and therefore was chosen for ΔK_{corr} analysis of the DED Type 304L material.

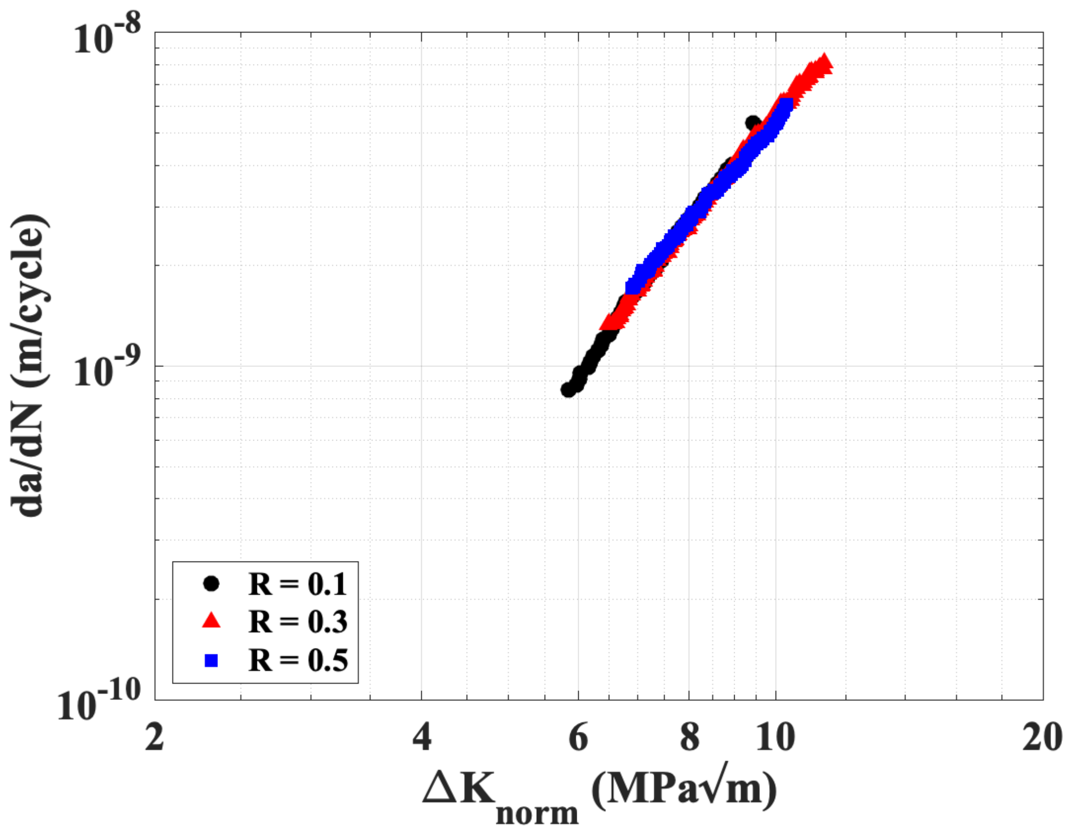

Figure 10: Fatigue crack growth rates (da/dN) vs ΔK_{norm} plots for normalization parameter of 0.25.

3.4. Fatigue Crack Growth Assessment of DED Type 304L

Values of R_{tot} (Eq. (2)) for the four ΔK decreasing and four ΔK increasing fatigue tests are shown in Figure 11. Compared to R_{app} of 0.1 (red line), R_{tot} is always greater. During the ΔK decreasing portion of the test, R_{tot} increases as K_{res} becomes a larger contributor relative to $K_{min,app}$ and $K_{max,app}$ (Equation 2). In the ΔK increasing portion of the test, K_{res} becomes a smaller contributor to R_{tot} because K_{res} decreases as the crack extends (Figure 6) and because the applied K values increase. Thus, R_{tot} trends toward R_{app} during the final stages of the test (a* > 17 mm).

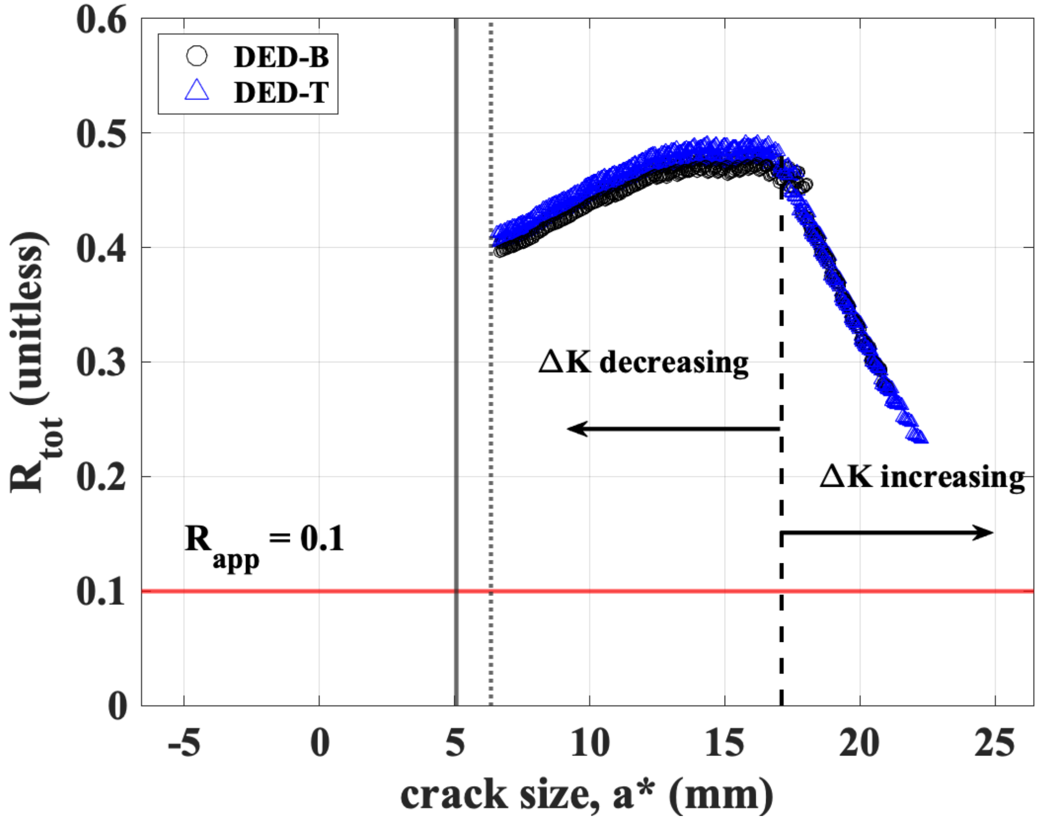

Figure 11: R_{tot} versus crack size for DED Type 304L stainless steel from all four decreasing and increasing ΔK_{app} fatigue tests using K_{res} from incremental slitting. The vertical lines represent the notch tip (solid line) and the end of the precrack region (dotted line) of fatigue crack growth.

3.5. Corrected Fatigue Crack Growth Data

Compliance data for wrought (Wrought1) and DED (DED2-B) specimens are shown in Figures 12(a) and 12(b) respectively. In wrought material with nominally zero residual stress, plasticity and roughness lead to crack face contact and a deviation from linearity in the compliance data. In contrast, for the DED material, the positive K_{res} mitigates crack closure by preventing crack face contact, thus ΔK_{ACR} is equal to ΔK_{app}.

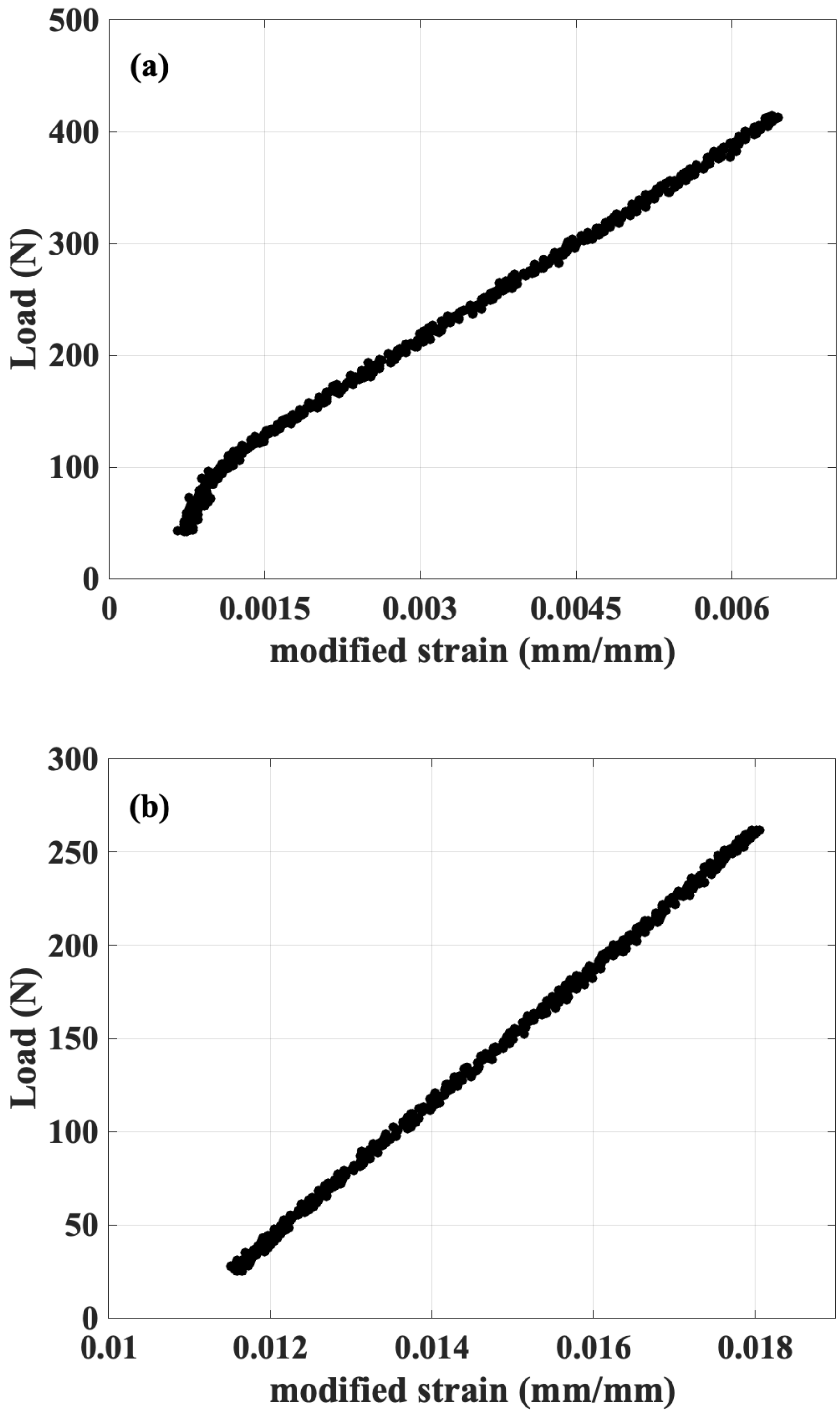

Figure 12: Compliance data for (a) wrought (Wrought1) Type 304/304L stainless steel showing deviation from linearity at $\Delta K_{app} = 4.9$ MPa$m^{0.5}$ and (b) DED (DED2-B) Type 304L stainless steel showing complete linearity at $\Delta K_{app} = 4.2$ MPa*$m^{0.5}$.*

To compare the intrinsic fatigue resistance of DED material to wrought material, fatigue crack growth data for DED material corrected for residual stress (ΔK_{corr}) are compared to fatigue crack growth data for wrought material corrected for crack closure (ΔK_{ACR}) in Figure 13. The wrought material has higher fatigue crack growth rates than observed in the DED material after correcting for closure and K_{res} respectively.

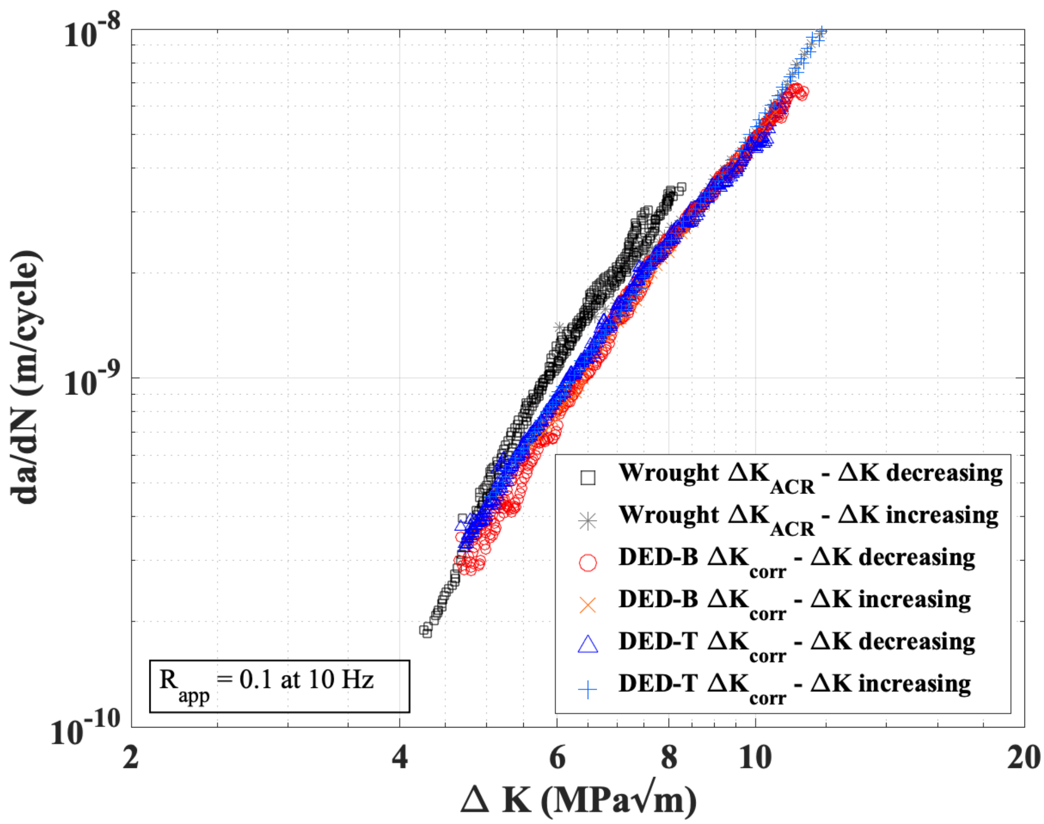

Figure 13: Fatigue crack growth rates (da/dN) vs ΔK_{corr} for DED 304L and ΔK_{ACR} for wrought 304/304L stainless steel.

4. *Discussion*

Residual stress profiles on multiple planes in the DED vertical wall build are consistent (Figure 4), suggesting that the residual stress in the build direction is relatively uniform along the height of the build. The lack of variability of residual stress with build height can be attributed to the refinement and careful control of depositon process parameters. Thus, residual stress in the test specimens is independent of the position of extraction from the build (i.e., bottom (B), middle (M), and top (T)), however, it does vary with position from the front face (x). As shown in Figure 5, the residual stress near the front face of the C(T) specimen is tensile, and becomes compressive towards the middle of the specimen and remains compressive near the back face. The temperature gradients of the deposited material result in rapid solidification of the surfaces and slower cooling rates of the center. As such, tensile residual stress is induced at the surface, which is balanced by compressive residual stress at the center as shown in the incremental slitting results of Figure 4. This figure highlights the high tensile residual stress at the as-built edges of the DED material, suggesting that if the slitting measurement in Figure 5 had been performed for the entirety of the C(T) specimen length (1.25W), the positions near the back face would return to large values of tensile residual stress.

The incremental slitting method measurements of DED1-M provided an estimate of K_{res}, which acts to drive crack growth in the DED material. The tensile residual stress at the edges of the builds led to positive values of K_{res} close to 4 $MPa \cdot m^{0.5}$ at the front face of the C(T) specimens after sample extraction. This positive value of $K_{res,}$ despite decreasing as the cut progressed through the residual stress field, is sufficient to maintain an open crack wake and accelerate measured fatigue crack growth rates. In the case of positive K_{res}, the net value of the stress intensity factor can be found using the superposition principle without complications of nonlinear crack face contact. That is, if the residual stress field is known, a net driving force for fatigue crack growth can be calculated during post fatigue testing analysis and the ΔK_{corr} method can be used to correct for the influence of residual stress on fatigue crack growth data.

Fatigue crack growth behavior from all four specimens of the two DED vertical wall builds agreed well with each other (Figure 8) and suggests repeatability in mechanical performance of AM materials manufactured with identical processing parameters. The differences between top and bottom specimens were negligible, especially when compared to the differences between AM and wrought. For all four C(T) specimens, the DED material displayed higher fatigue crack growth rates in the near threshold regime for equal applied ΔK as compared to the stress-free wrought Type 304/304L (Figure 8). This difference in fatigue crack growth rate is associated with tensile residual stress and the resulting effects on R_{tot} from the variation of K_{res} and the evolution of ΔK_{app}. The positive K_{res} from the tensile residual stress in DED material led to values of R_{tot} that were higher than the applied stress ratio, R_{app}, of 0.1 for the duration of the fatigue tests. Figure 11 demonstrates that at the low applied ΔK values as the ΔK decreasing test approached the threshold for fatigue crack growth, R_{tot} for the DED tests was close to 0.5, which is significantly different from R_{app} of 0.1. Typically, higher R (for the same ΔK) leads to higher fatigue crack growth rates. This is the principal reason that the crack growth rates are higher in the DED material than in the wrought material at the same values of ΔK_{app}.

Subtle differences between the apparent fatigue crack growth rates are also evident in the ΔK decreasing and ΔK increasing portions of the tests in the DED material. These differences can be attributed to the evolution of K_{res} throughout the specimen. In the initial ΔK decreasing portion of the fatigue crack growth tests, K_{res} is maximum with a shallow slope (Figure 6), thus the apparent fatigue crack growth rates exhibit the largest effect from residual stress in this region. In the ΔK increasing portion, however, the positive K_{res} values are less than in the initial stages of crack growth and the apparent fatigue crack growth rates are slower than those of the ΔK decreasing (initial) portion of the test. In the absence of residual stress, the wrought material ΔK decreasing and ΔK increasing portions of the test resulted in consistent fatigue crack growth rates. Therefore, the differences in apparent fatigue crack growth rates of the DED material are associated with the varying K_{res} profile of the DED material. In the absence of crack face contact, the intrinsic fatigue resistance of the DED material can be estimated from the ΔK_{corr} (Equation 5) with ΔK_{eff} equal to ΔK_{app}. For a material with negligible residual stress, R_{app} is equal to R_{tot} for the duration of the fatigue test and ΔK_{corr} is not applicable. Therefore, for the wrought material, post testing analysis is limited to adjusting for crack face contact using ΔK_{ACR}.

The fatigue crack growth rate data are corrected for the influence of process induced bulk residual stress when plotted as a function of ΔK_{corr}. To compare the intrinsic behavior of the DED and wrought materials, the corrected fatigue crack growth data (ΔK_{corr}) of the DED material are plotted with the ΔK_{ACR} of the wrought material in Figure 13. The fatigue crack growth rate data for the DED material agree, confirming that the differences between the apparent fatigue crack growth rate data were due to the influence of residual stress. Here, the apparent fatigue threshold for DED material if the current trend is projected to a threshold crack growth rate as defined by the ASTM standard (10^{-10} m/cycle) appears to be similar to that of the wrought material at about 4 MPa·$m^{0.5}$ (Figure 13). DED and wrought fatigue crack growth rate data converge when both materials have been corrected for residual stress and crack closure respectively, suggesting that the intrinsic fatigue resistance of the two materials are similar near threshold. However, for higher fatigue crack growth rates (>10^{-9} m/cycle) and values of ΔK greater than 6 MPa·$m^{0.5}$, the DED material exhibits slightly lower fatigue crack growth rates as compared to wrought material.

5. Conclusions

The residual stresses and unique microstructures formed by high cooling rates and thermal gradients of the manufacturing process are expected to influence apparent fatigue crack growth rates in AM materials in their as-built state as compared to their wrought counterparts.

The present study focused on developing a quantitative understanding of the impact of residual stress on fatigue cracking to evaluate the intrinsic differences between AM and wrought 304/304L materials. The key conclusions are:

1. The results show that near-threshold fatigue crack growth rates in DED Type 304L are influenced significantly by the presence of tensile residual stress. Specifically, for the specimens extracted from the as-built DED Type 304L stainless steel in this study, fatigue crack growth rates were measured to be 3.5 times faster than in commercially available wrought Type 304/304L stainless steel in the near threshold regime ($<10^{-8}$ m/cycle) at an applied ΔK of 5 $MPa \cdot m^{0.5}$.
2. The residual stress intensity factor, K_{res}, determined from incremental slitting experiment data of both DED and wrought materials revealed positive values ranging from 4 $MPa \cdot m^{0.5}$ at the notch tip to 1 $MPa \cdot m^{0.5}$ at the end of fatigue crack growth for DED Type 304L; in contrast, the wrought material displayed negligible residual stress.
3. The DED Type 304L did not exhibit crack closure, which is consistent with the positive applied stress ratio and positive values of K_{res}. In contrast, the effects of crack closure were present in the data for wrought Type 304/304L, consistent with negligible K_{res}.
4. The DED Type 304L stainless steel and the wrought Type 304/304L exhibited similar intrinsic fatigue crack growth rates when the DED Type 304L data were corrected for residual stress using the ΔK_{corr} method and the wrought Type 304/304L data were adjusted for the effects of crack closure using the adjusted compliance ratio (ΔK_{ACR}). This comparison demonstrates that the different apparent fatigue crack growth rates

of DED and wrought material can be attributed to the combination of residual stress and crack closure, which are different in these two materials.

5. While similar, corrected crack growth rates in DED Type 304L were slightly lower than those in wrought Type 304/304L. The lower fatigue crack growth rates are hypothesized to be related to the unique microstructure (grain size and morphology) of the DED material, which had a small influence on its intrinsic fatigue crack growth resistance compared to the more significant impact of residual stress.

Acknowledgements:

This work was supported by a NASA Space Technology Research Fellowship (CMS) and material was provided by Sandia National Laboratories. Sandia National Laboratories is a multi-mission laboratory managed and operated by National Technology & Engineering Solutions of Sandia, LLC, a wholly owned subsidiary of Honeywell International Inc., for the U.S. Department of Energy's National Nuclear Security Administration under contract DE-NA0003525. This paper describes objective technical results and analysis. Any subjective views or opinions that might be expressed in the paper do not necessarily represent the views of the U.S. Department of Energy or the United States Government.

References:

1. Yadollahi, A. and N. Shamsaei, *Additive manufacturing of fatigue resistant materials: Challenges and opportunities.* International Journal of Fatigue, 2017. **98**: p. 14-31.
2. Fatemi, A., et al., *Fatigue behaviour of additive manufactured materials: An overview of some recent experimental studies on Ti-6Al-4V considering various processing and loading direction effects.* Fatigue & Fracture of Engineering Materials & Structures, 2019. **42**(5): p. 991-1009.
3. Mishurova, T., et al., *Separation of the impact of residual stress and microstructure on the fatigue performance of LPBF Ti-6Al-4V at elevated temperature.* International Journal of Fatigue, 2021. **148**.
4. Anderson, T.L., *Fracture Mechanics: fundamentals and applications.* CRC Press, 2005. **Chapter 10: Fatigue Crack Propagation**(Third Edition).
5. Daniewicz, S.R. and N. Shamsaei, *An introduction to the fatigue and fracture behavior of additive manufactured parts.* International Journal of Fatigue, 2017. **94**: p. 167-167.
6. Shamsaei, N. and J. Simsiriwong, *Fatigue behaviour of additively-manufactured metallic parts.* 3rd International Symposium on Fatigue Design and Material Defects (Fdmd 2017), 2017. **7**: p. 3-10.
7. Riemer, A., et al., *On the fatigue crack growth behavior in 316L stainless steel manufactured by selective laser melting.* Engineering Fracture Mechanics, 2014. **120**: p. 15-25.
8. Riemer, A. and H.A. Richard, *Crack Propagation in Additive Manufactured Materials and Structures.* 21st European Conference on Fracture, (Ecf21), 2016. **2**: p. 1229-1236.
9. Leuders, S., et al., *On the mechanical behaviour of titanium alloy TiAl6V4 manufactured by selective laser melting: Fatigue resistance and crack growth performance.* International Journal of Fatigue, 2013. **48**: p. 300-307.
10. Gordon, J.V., et al., *Fatigue crack growth anisotropy,texture and residual stress in austenitic steel made by wire and arc additive manufacturing.* Materials Science and Engineering a-Structural Materials Properties Microstructure and Processing, 2018. **724**: p. 431-438.
11. Ran, X.-z., et al., *Effects of microstructures on the fatigue crack growth behavior of laser additive manufactured ultrahigh-strength AerMet100 steel.* Materials Science and Engineering: A, 2018. **721**: p. 251-262.
12. Rangaswamy, P., et al., *Residual stresses in LENS (R) components using neutron diffraction and contour method.* Materials Science and Engineering a-Structural Materials Properties Microstructure and Processing, 2005. **399**(1-2): p. 72-83.
13. Donald, J.K. and D.A. Lados, *An integrated methodology for separating closure and residual stress effects from fatigue crack growth rate data.* Fatigue & Fracture of Engineering Materials & Structures, 2006. **30**(3): p. 223-230.
14. James, M., et al., *A Methodology for Partitioning Residual Stress Effects From Fatigue Crack Growth Rate Test Data.* Materials Performance and Characterization, 2016. **5**(3).
15. Ronevich, J.A., C.R. D'Elia, and M.R. Hill, *Fatigue crack growth rates of X100 steel welds in high pressure hydrogen gas considering residual stress effects.* Engineering Fracture Mechanics, 2018. **194**: p. 42-51.
16. *E647-15e1 Standard Test Method for Measurement of Fatigue Crack Growth Rates.* ASTM International, 2015.

17. Smith, T.R., et al., *Effects of Extreme Hydrogen Environments on the Fracture and Fatigue Behavior of Additively Manufactured Stainless Steels.* Proceedings of the ASME 2019 Pressure Vessels & Piping Conference, 2019. **PVP 2019-93903**.
18. *A240/A240M-19 Standard Specification for Chromium and Chromium-Nickel Stainless Steel Plate, Sheet, and Strip for Pressure Vessels and for General Applications*. 2019, ASTM International: West Conshohocken, PA.
19. Hill, M.R., *Chapter 4: The Slitting Method*, in *Practical Residual Stress Measurement Methods*, G.S. Schajer, Editor. 2013, Wiley. p. 89-108.
20. Schajer, G.S. and M.B. Prime, *Use of inverse solutions for residual stress measurements.* Journal of Engineering Materials and Technology-Transactions of the Asme, 2006. **128**(3): p. 375-382.
21. Schindler, H.J., W. Cheng, and I. Finnie, *Experimental determination of stress intensity factors due to residual stresses.* Experimental Mechanics, 1997. **37**(3): p. 272-277.
22. Olson, M.D. and M.R. Hill, *Determination of residual stress intensity factor in the compact tension coupon.* Engineering Fracture Mechanics, 2012. **88**: p. 28-34.
23. Donald, J.K., G.H. Bray, and R.W. Bush, *An evaluation of the adjusted compliance ratio technique for determining the effective stress intensity factor.* Fatigue and Fracture Mechanics: Twenty-Ninth Volume, 1999. **1332**: p. 674-695.
24. Dowling, N.E., *Mechanical behavior of materials : engineering methods for deformation, fracture, and fatigue*. 4th ed. 2013, Boston: Pearson. xvii, 936 p., Chapter 9: 416-490.
25. Rasband, W.S., *ImageJ.* U. S. National Institutes of Health.